Computational analysis of adhesion force in the indentation of cells using atomic force microscopy

C. Y. Zhang and Y. W. Zhang*

Department of Materials Science and Engineering, National University of Singapore, Singapore 119260

(Received 19 July 2007; published 21 February 2008)

A mechanical model was developed to study the indentation of an atomic force microscopic (AFM) tip on a cell with adhesion mediated by receptor-ligand binding. The effects of indentation rate, indentation depth, indenter size, and the mechanical properties of cells on the adhesion force were investigated. It was found that the presence of adhesion between the cell and AFM tip may affect both the loading curve and unloading curve, which may in turn change the extracted elastic modulus values using the conventional indentation models. It was found that an increase in the receptor-ligand reaction rate may lead to a transition from a decrease of the maximum adhesion force with the indentation rate to an increase of the maximum adhesion force with the indentation rate. It was also found that factors such as indenter size, indentation depth, and cell mechanical properties influence the maximum adhesion force, and their corresponding underlying mechanisms were discussed.

DOI: 10.1103/PhysRevE.77.021912 PACS number(s): 87.15.K−, 68.35.Np, 87.15.La, 62.25.−g

I. INTRODUCTION

Adhesion of a cell to another cell or to an extracellular matrix is of great importance in many biological processes and biotechnological applications [1,2]. Indentation using atomic force microscopy (AFM) has been emerging as a powerful technique to study the biological and mechanical behavior of living cells due to its capability of characterizing both the mechanical response of cells [3–5] and the cellular adhesion behavior as well [6–8]. By pushing an AFM tip (or a microbead attached to the end of the cantilever [8]) against a sample to a certain depth and then retracting it, a complete force-indentation curve can be collected. By using an appropriate indentation model, the mechanical properties of cells may be determined from the indentation loading curve, and the adhesion behavior may be obtained from the unloading curve. There are several advantages in using this technique: the ability to maintain cell viability, the possibility of local measurement, relatively precise force determination, and repeatability.

Conventionally, the extraction of mechanical properties of cells by contact models such as the Hertz theory [9] or the Sneddon solution [10] does not consider cell adhesion. Thus whether or not such extraction is affected by the adhesion force is yet unclear. In addition, the adhesion force may also be affected by many experimental parameters, such as the indentation rate, indentation depth, and the geometry of the indenter. Therefore understanding of the effects of those system parameters on the adhesion force is necessary to reliably measure the cellular adhesion strength.

Certain progress has been made toward understanding the receptor-ligand mediated cell adhesion, and so far, several mathematical models have been proposed to describe the adhesion process based either on the equilibrium concept [11,12] or on the kinetics concept [13,14]. Those kinetic models applied chemical reaction equations to describe the receptor-ligand binding and unbinding events. Other simulation techniques, such as probabilistic and Monte Carlo methods, have also been applied to study cell adhesion [15]. The kinetic approach has been successfully applied to model the transient response of cell adhesion in flow [16–20]. However, their applications to cell adhesion in the AFM indentation have not been attempted.

In the present study, we employed a kinetic approach to model the cell-indenter adhesion. One major computational challenge of using kinetic models was to bridge the disparate length scale between the cell (on an order of μm) and the receptor-ligand bonds (on an order of nm). Here a continuum-kinetics framework was formulated, which was able to simultaneously describe the deformation of cells and the cell-indenter adhesion.

II. THEORETICAL FORMULATION

A. Constitutive response of cells

Cells often exhibit viscoelastic behavior. Although membranes have long been assumed to behave elastically under stretching and bending, the mechanisms responsible for the viscoelastic behaviors of cells are yet not fully understood. Previous studies have attributed the viscoelastic behavior to various reasons, for example, to the intrinsic viscoelasticity of the cytoplasm [21–23], or to the biphasic effect arising from fluid-solid interaction within the cell [24], or to both (poroviscoelasticity [25]). A recent study indicated that the cell viscoelasticity is also sensitive to the measurement frequency [26]: at a low frequency (time domain), the viscoelasticity characterized by an exponential law dominates; while at a high frequency (frequency domain), a nonlinear viscoelasticity characterized by a power law dominates. At the time domain, it was also found that a simple viscoelastic model (a compressible neo-Hookean model in parallel with a Maxwell model) could predict many features of a cell's creep response [27]. Since the present study is limited to the measurements in the time domain, a similar model was adopted

*Corresponding author. FAX: 65-67763604. msezyw@nus.edu.sg

to describe the viscoelastic behavior of cells: to capture the large deformation response of cell membranes, the composite membrane (comprising the phospholipid bilayer, the underlying spectrin network, and transmembrane proteins) was modeled as an effective hyperelastic layer [28,29] and the cytoplasm was idealized as a simple viscoelastic neo-Hookean solid.

In the first-order formulation, the strain energy potential of the effective hyperelastic membrane takes the following neo-Hookean form:

$$U = \frac{\mu_0}{2}(I_1 - 3) + \frac{K_0}{2}(J-1)^2, \tag{1}$$

where U is the strain energy per unit reference volume, μ_0 and K_0 are the initial shear modulus and bulk modulus, respectively, I_1 is the first deviatoric strain invariant, and J is the elastic volume ratio.

The shear deformation of cytoplasm was assumed to be described by the viscoelastic neo-Hookean model. Its dimensionless shear relaxation modulus can be expressed by a Prony series expansion,

$$\bar{\mu}_R(t) \equiv \frac{\mu_R(t)}{\mu_0^s} = 1 - \sum_{i=1}^{N} \bar{\mu}_i(1 - e^{-t/\tau_i}), \tag{2}$$

where $\mu_R(t)$ is the shear relaxation modulus, $\bar{\mu}_i$ and τ_i $(i=1,2,\ldots N)$ are the material constants, and μ_0^s is the initial shear modulus of the cytoplasm, i.e., $\mu_R(0)$. The volumetric deformation was assumed to be elastic. To account for the limited compressibility of cells [21,27], the Poisson ratio $v=0.49$ was assumed for both the membrane and the cytoplasm. The Poisson ratio ν relates to μ_0 and K_0 by $\nu=(3K_0/\mu_0-2)/(3K_0/\mu_0+2)$.

B. Kinetic model for receptor-ligand reaction

The binding and unbinding between the receptors on the cell surface and the ligands on the indenter surface was assumed to be governed by a chemical reaction in which a receptor (R) and a ligand (L) can form a bond (B) [2],

$$[R] + [L] \underset{kr}{\overset{kf}{\leftrightarrow}} [B], \tag{3}$$

where $[R]$, $[L]$, and $[B]$ are the densities of the receptors, the ligands, and the receptor-ligand bonds, respectively; k_f and k_r are the forward and reverse reaction rates, respectively. The density of the receptor-ligand bonds is governed by a simple kinetic relationship:

$$\frac{d[B]}{dt} = k_f([L_0]-[B])([R_0]-[B]) - k_r[B]$$
$$\approx k_{on}([R_0]-[B]) - k_r[B] \quad \text{when } [L_0] \gg [R_0], \tag{4}$$

where $[R_0]$ and $[L_0]$ are the initial densities of the receptors and the ligands, respectively. Since typical receptor densities are usually low on the cell membrane surface [16], for simplicity, we focus on the low receptor regime. Thus when $[L_0] \gg [R_0]$, $k_{on} \equiv k_f[L_0]$. It has been shown that the adhesion is dependent on the magnitude of the externally applied force, and therefore the reaction rates are also force dependent [11–14]. Motivated by this force dependency of the binding and unbinding rates, several models have been proposed to describe the receptor-ligand reaction [11,14,20]. Here we follow Dembo *et al.*'s model and treat the receptor-ligand bond as a linear spring with a spring constant σ and a natural length λ [14]. This model has been successfully applied to simulate cell rolling and adhesion on extracellular surfaces [16,17], cell adhesion and movement in fluid [19], and the detachment of macromolecularly bound particles from extracellular surfaces [30]. In this model, $k_f = k_f^0 \exp\left(\frac{\sigma_{ts}(x_m-\lambda)^2}{2k_BT}\right)$ and $k_r = k_r^0 \exp\left(\frac{(\sigma-\sigma_{ts})(x_m-\lambda)^2}{2k_BT}\right)$, where k_f^0 and k_r^0 are the intrinsic forward and reverse reaction rates, respectively; x_m is the intermolecular separation, σ_{ts} is the transition state spring constant, and k_BT is the product of the Boltzmann constant and the absolute temperature. It can be seen that when the intermolecular separation is equal to the bond nature length, that is, $x_m=\lambda$, we have $k_f=k_f^0$ and $k_r=k_r^0$. Since the receptor-ligand binding was described by the simple first-order chemical reaction equation [Eq. (4)], the time rate of the receptor-ligand bonds density is proportional to the density of receptors. Hence it can be deduced that the adhesion force may increase proportionally with the density of receptors.

C. Computational model

In the present study, the indentation of a cell was modeled as that of a soft half space (described by the viscoelastic neo-Hookean model) covered by a film with a thickness of h (described by the hyperelastic neo-Hookean model). For simplicity, only one time scale [i.e., $N=1$ in Eq. (2)] was included in the viscoelastic material. In the indenter-cell contact region, the compressive contact force was calculated by using the standard penalty algorithm [31]. The interaction force between the indenter and the cell surface per unit area, T_B, was calculated through

$$T_B = [B](x_m - \lambda)\sigma, \tag{5}$$

where the bond density $[B]$ was obtained by solving Eq. (4). Here a continuous evolution of the bond density was assumed. Therefore the method should work well for large-scale adhesion such as the indentation using microbeads (with a size on an order of μm) [8,32], but might smooth the multiple-step breakage of the receptor-ligand bonds in small-scale adhesion such as the indentation using commercial AFM tips (with a size on an order of nm) [5,7,16,30].

An axisymmetric finite element model was formulated by using the general-purpose finite element (FE) code ABAQUS/EXPLICIT V6.6 (Providence, RI) (Fig. 1, left). The ligands were assumed to be uniformly coated on the rigid spherical indenter (radius=R) and the receptors were assumed to be uniformly distributed on the cell membrane. The interaction (both compression and attraction) between the indenter and the cell was defined by writing a user-defined subroutine embedded into the ABAQUS code. It should be mentioned that other kinetic models describing the receptor-ligand binding

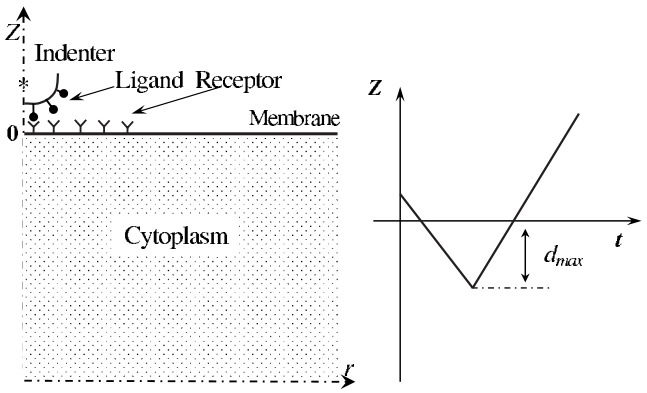

FIG. 1. Schematic of the axisymmetric finite element model for cell indentation (left); movement of the indenter with reference to $z=0$ being the top surface of the membrane (right).

[11,14,20,33] can also be implemented within the same framework.

III. RESULTS AND DISCUSSION

Parametric studies were conducted to investigate the influence of indentation parameters on adhesion forces and further the influence of adhesion forces on indentation curves. The rigid spherical indenter was pressed onto the sample and then retracted with a controlled velocity, $\dot{z}$, (Fig. 1, right). The electrostatic interaction and steric repulsion between the cell and the tip were assumed to be absent. In the following sections, the horizontal axis of the indentation curves represents the position of the spherical indenter with reference to $z=0$, which is the top surface of the cell. The materials and system parameters used in the calculations are listed in Table I. The same set of parameters were used throughout the study unless stated otherwise.

A. Influence of adhesion force on indentation curves

Figures 2(a) and 2(b) compare the indentation curves with and without adhesion at two different receptor-ligand reaction rates. Typical materials and system data listed in Table I were used. The result for the higher receptor-ligand reaction rate with $k_f^0=1.0\times10^2$ s^{-1} μm^2 and $k_r^0=1.0\times10^{-2}$ s^{-1} is shown in Fig. 2(a) while the result for the lower receptor-ligand reaction rate with $k_f^0=1.0\times10^{-2}$ s^{-1} μm^2 and $k_r^0=1.0\times10^{-6}$ s^{-1} is shown in Fig. 2(b). Two types of depen-

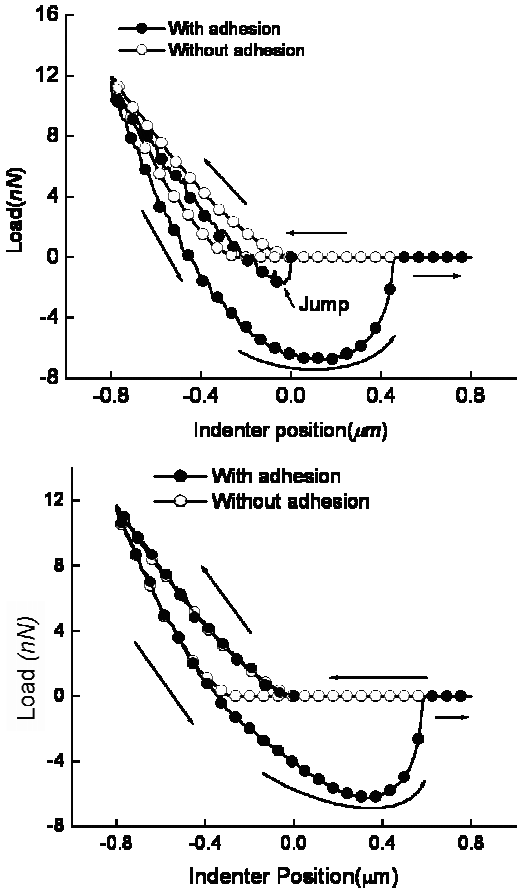

FIG. 2. Influence of cell adhesion on indentation curves. (a) a fast receptor-ligand reaction; (b) a slow receptor-ligand reaction.

TABLE I. Materials and system parameters used in the present calculations.

Parameter	Symbol	Value
Initial shear modulus of cell membrane	μ_0^f	~2.0 M Pa [28]
Initial shear modulus of cytoplasm	μ_0^s	1.0–30.0 K Pa [5]
Coefficient of Prony series expansion	$\bar{\mu}_1$	0.9 [23]
Viscoelastic time scale	τ_1	~1.0 s [21,23,27]
Indenter radius	R	0.5–6.0 μm [32]
Indentation velocity	$\dot{z}$	0.125–2.5 μm/s [5]
Thickness of cell membrane	h	~10.0 nm
Natural length of bond	λ	20.0 nm [30]
Intrinsic forward reaction rate	k_f^0	1.0×10^{-4}–1.0×10^2 s^{-1} μm^2 [16,30]
Intrinsic reverse reaction rate	k_r^0	1.0×10^{-9}–1.0×10^{-2} s^{-1} [16,30]
Initial receptor density	$[R_0]$	~10.0 μm^{-2} [16]
Initial ligand density	$[L_0]$	~1.0×10^3 μm^{-2} [16]
Spring constant	σ	1.0–2.0 dyne/cm [16]
Transition state spring constant	σ_{ts}	0.0–2.0 dyne/cm [16]

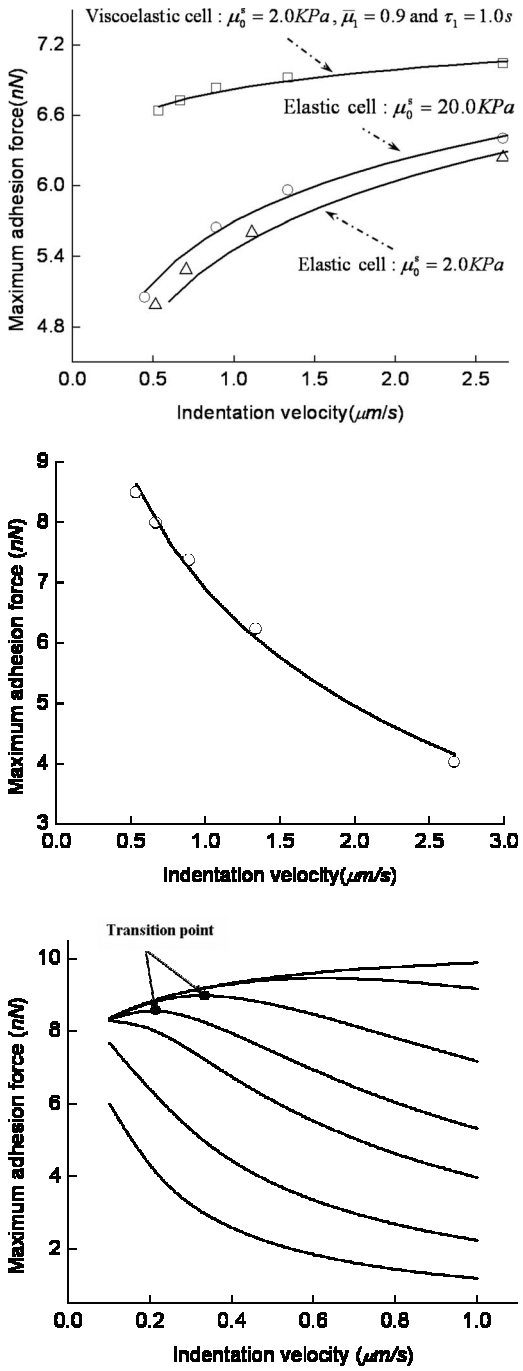

FIG. 3. Influence of indentation rate on maximum adhesion force. (a) maximum adhesion force increases with indentation velocity; (b) maximum indentation force decreases with indentation velocity [for (a) and (b), hollow symbols represent computational results; solid lines represent fitting curves]; (c) reaction rate-controlled transition of the scaling relation. From the uppermost to the lowermost curves, the binding rates are $k_f^0 = 2.0 \times 10^{-2}$ s^{-1} μm^2, 1.0×10^{-2} s^{-1} μm^2, 5.0×10^{-3} s^{-1} μm^2, 3.0×10^{-3} s^{-1} μm^2, 2.0×10^{-3} s^{-1} μm^2, 1.0×10^{-3} s^{-1} μm^2, 5.0×10^{-4} s^{-1} μm^2.

dency of the indentation loading curve on the receptor-ligand reaction rate were observed in the presence of adhesion: If the receptor-ligand reaction is fast, the influence of the adhesion on the indentation loading curve is significant. However, if the receptor-ligand reaction is slow, the influence of the adhesion force becomes insignificant. These observations may be explained by the fact that the total indentation force can be decomposed into two parts: the contact force and the adhesion force. For the conventional indentations (without adhesion), only contact force is present. For the indentations with adhesion, however, the contact force exists in the contact zone in which the receptor-ligand bonds are in compression while the adhesion force exists in the adhesion zone in which the receptor-ligand bonds are in tension. During the indentation loading process, the contact zone grows with an increase in the indentation depth. Meanwhile the adhesion zone which is in a ring shape enclosing the contact zone also expands outwards with the growth of the contact zone. Hence the number of bonds formed during the transient period, that is, from the formation of an adhesion zone to its transformation into a contact zone, strongly influences the cell adhesion: A higher reaction rate leads to a larger number of bonds formed whereas a lower reaction rate leads to a smaller number of bonds formed. Therefore the contribution of the adhesion force to the total indentation force is significant for the former while insignificant for the latter. Since the cell elastic modulus is conventionally extracted by fitting the loading curve [3–5], it is expected that the influence of adhesion force on cell modulus extraction is significant for the former while insignificant for the latter. When the receptor-ligand reaction is fast, the loading curve is complicated by a jump-to-contact phenomenon as shown in Fig. 2(a). This phenomenon is due to the attractive forces caused by the fast formation of receptor and ligand bonds [34]. It can be seen from Fig. 2(a) that the jump-to-contact phenomenon increases the loading curve slope. Hence the conventional extraction of cell elastic modulus by fitting the loading curve may significantly overestimate its value if the jump-to-contact phenomenon is not considered. In practical indentation tests, other factors, such as the electrostatic and steric repulsions between the cell and the ligand-coated tip [35], may also complicate the extraction of cell elastic modulus.

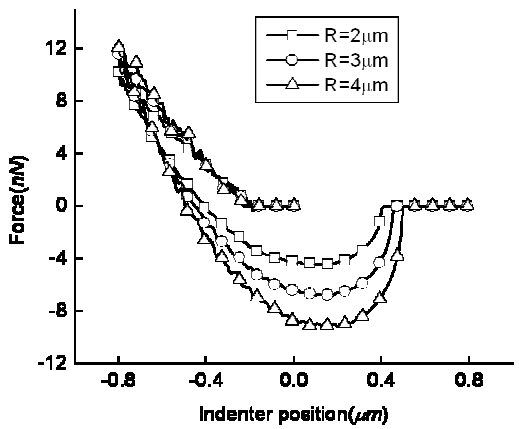

FIG. 4. Influence of indenter radius on adhesion force.

The influence of adhesion on the unloading curves is evident in Figs. 2(a) and 2(b). It can be seen that cell adhesion significantly tilts the indentation unloading curves downwards. During the retraction, the adhesion interaction ex-

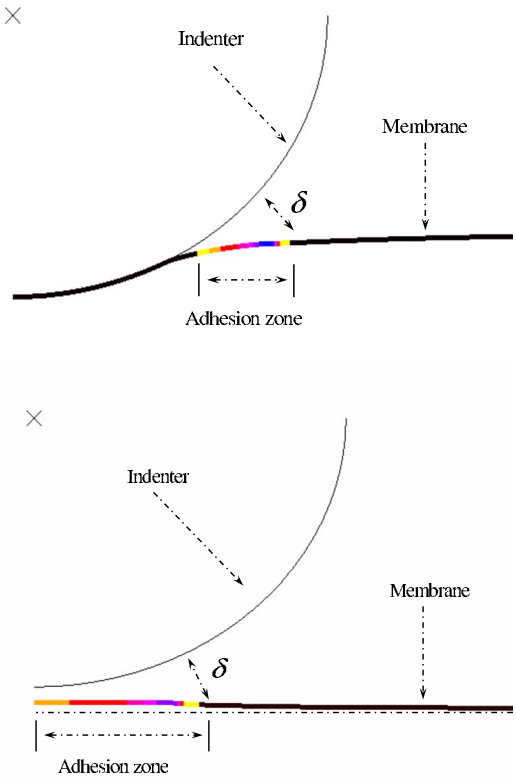

FIG. 5. (Color online) (a) Schematic of the adhesion zone and contact zone; (b) the contact zone vanishes and the adhesion zone is completely dominant during the retraction process.

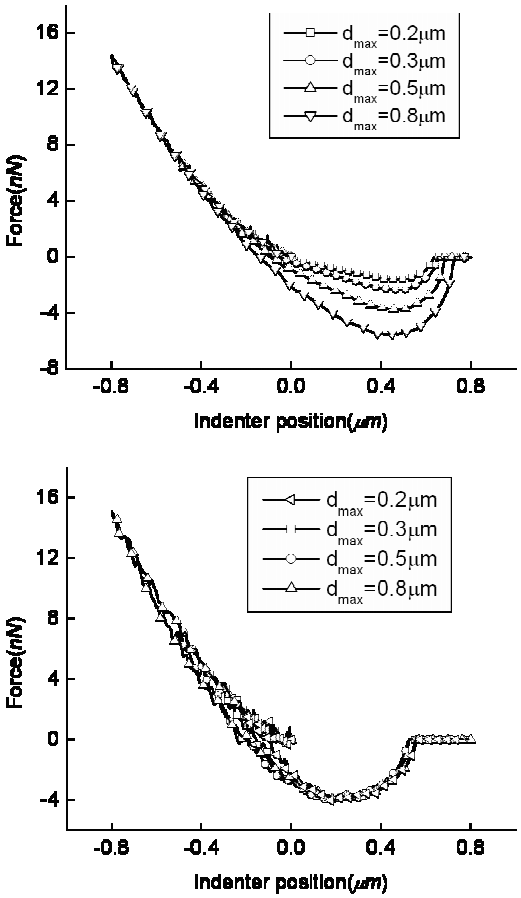

FIG. 6. Influence of indentation depth on adhesion force of an elastic cell with $\mu_0^s=2.0$ K Pa. (a) A low receptor-ligand reaction rate with $k_f^0=1.0\times10^{-2}$ s^{-1} μm^2 and $k_r^0=1.0\times10^{-6}$ s^{-1}.(b) A high receptor-ligand reaction rate with $k_f^0=1.0\times10^{2}$ s^{-1} μm^2 and $k_r^0=1.0\times10^{-2}$ s^{-1}.

tends far beyond the initial contact point during the loading process, giving rise to a large hysteresis loop [see Fig. 2(b)]. For the viscoelastic cell without cell adhesion, however, the unloading curve tilts downwards only slightly compared with the case with cell adhesion, indicating that the contribution of cell viscoelasticity to the hysteresis loop is relatively small [see Fig. 2(a)]. Since the maximum adhesion force and the hysteresis loop area are primarily related to adhesion properties, relations between these quantities may be useful for extracting the adhesion properties. Hence an important future work will be to establish these relations.

B. Influence of indentation velocity on adhesion force

The receptor-ligand reaction (binding and unbinding) is a kinetic process, implying that the adhesion force may depend on the magnitude of $\dot{z}$, the indentation rate [11–15,30]. So far, experimental results have shown two types of dependency of the maximum adhesion force on the indentation rate: (i) the maximum adhesion force increases with an increase in the indentation rate [11,36–39]; (ii) the maximum adhesion force decreases with an increase in the indentation rate [8]. The reason for the discrepancy in these experimental observations is not yet clear.

In order to understand the underlying reason, parametric studies were performed by varying both the forward reaction rate (or the binding rate) k_f^0 and the indentation rate $\dot{z}$ while keeping the reverse reaction rate (or the unbinding rate) fixed at $k_r^0=1.0\times10^{-6}$ s^{-1}. The variation of the maximum adhesion force with the indentation rate at $k_f^0=2.0\times10^{-2}$ s^{-1} μm^2 was shown in Fig. 3(a). It is seen that for both the elastic (hollow triangles: elastic parameter $\mu_0^s=2.0$ K Pa; hollow circles: elastic parameter $\mu_0^s=20.0$ K Pa) and viscoelastic (hollow squares: viscoelastic parameters $\mu_0^s=2.0$ K Pa, $\bar{\mu}_1=0.9$, and $\tau_1=1.0$ s) cells, the maximum adhesion forces increase with the indentation rate, confirming the existence of the first type of dependency. Apparently this dependency is due to the kinetics of the receptor-ligand bond formation, not due to the cell viscoelasticity since the adhesion forces of the two elastic cells show the same tendency as that of the viscoelastic cell. The second type of dependency, i.e., the adhesion force decrease with an increase in the loading rate, was also captured if a low receptor-ligand binding rate was used. An example of this type of dependency is shown in Fig. 3(b) with $k_f^0=5.0\times10^{-4}$ s^{-1} μm^2. From Fig. 3(b), it is seen that the maximum adhesion force decreases with the indentation rate, confirming the existence of the second type of dependency.

The origin of the two types of loading rate dependency of the maximum adhesion force may be attributed to the difference in the reaction rate of the receptor-ligand bond formation with respect to the indentation rate. If the receptor-

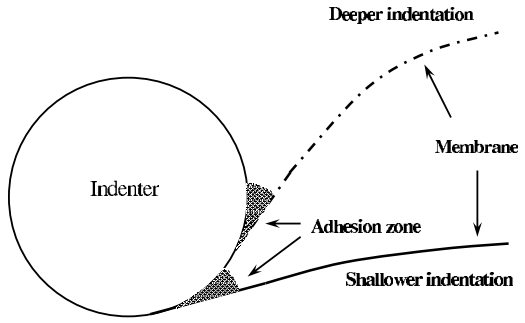

FIG. 7. Insensitivity of adhesion zone profile to the indentation depth due to a fast receptor-ligand reaction rate.

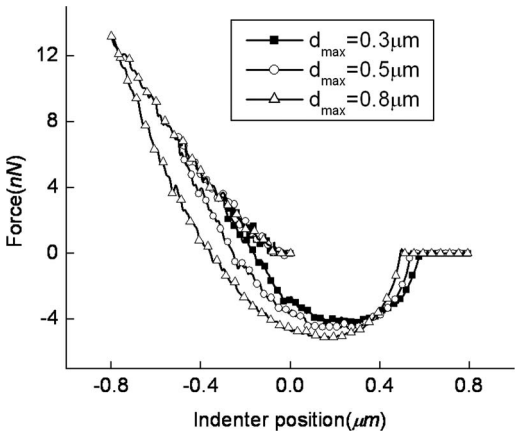

FIG. 8. Influence of indentation depth on adhesion force of a viscoelastic cell with $\mu_0^s=2.0$ K Pa, $\bar{\mu}_1=0.9$, and $\tau_1=1.0$ s. A high receptor-ligand reaction rate with $k_f^0=1.0\times10^2$ s^{-1} μm^2 and $k_r^0=1.0\times10^{-2}$ s^{-1} was used.

ligand binding is fast (compared with the indentation rate), the formation of the adhesive bonds will be insensitive to the indentation rate because the bonds can form almost instantaneously once a receptor and a ligand are in close proximity. Therefore the adhesion force is controlled by the relative magnitude of the unbinding rate and the indentation rate. A faster indentation unloading renders fewer *existing* receptor-ligand bonds to break before reaching the maximum adhesion force, causing a larger maximum adhesion force. This leads to the first-type dependency. However, if the binding rate is low (compared with the indentation rate), the formation of the adhesive bonds is unsaturated and a slower indentation unloading or a longer holding process will render more *new* bonds to form. Therefore the adhesion force increases with a decrease in the indentation rate. This leads to the second type of dependency. Our calculation results also showed that there might be a transition from one type of dependency to the other type. With a fixed unbinding rate, the transition was controlled by the binding rate as shown in Fig. 3(c). It is expected that different receptor-ligand pairs may have different reaction rates, which may lead to a complicated dependency between the adhesion force and indentation rate.

C. Influence of indenter size and indentation depth on adhesion force

Our simulation results showed that the adhesion force of a cell increases with an increase in the radius of indenter (Fig. 4. The present analysis suggested that the adhesion was not controlled by the actual contact area. The underlying reason is that the receptor-ligand bonds which contribute to the adhesion force are located only in the adhesion zone enclosing the contact zone [the adhesion zone size for $R=3$ μm is shown in Fig. 5(a)]: The bonds located within the contact zone serve just as internal contact springs and thus do not contribute to the adhesion force; while outside the adhesion zone, however, the separation between the receptors and ligands, δ, is too large to form bonds [see Fig. 5(a)]. The adhesion zone moves outward when the indenter is pressed onto a cell and moves inward when the indenter is retracted from the cell. At some moment during the retraction process, the contact zone vanishes and the interaction between the indenter and the cell is completely dominated by the adhesion zone. This moment for the case $R=3$ μm is captured in Fig. 5(b). It is seen that a larger indenter leads to a wider adhesion zone, which in turn leads to a larger adhesion force.

Figure 6 shows the indentation data of an elastic cell at the same indentation rate of $\dot{z}=1.6$ μm/s but at different indentation depths. For the elastic cell at a low receptor-ligand reaction rate, the maximum adhesion force increases with an increase in the maximum indentation depth. Examples are shown in Fig. 6(a) in which $k_f^0=1.0\times10^{-2}$ s^{-1} μm^2 and $k_r^0=1.0\times10^{-6}$ s^{-1}. With further increase in the reaction rate, the maximum adhesion force gradually saturates. Examples at the saturation stage are shown in Fig. 6(b) in which $k_f^0=1.0\times10^2$ s^{-1} μm^2 and $k_r^0=1.0\times10^{-2}$ s^{-1}. In these calculations, the affinity, which is defined as the ratio of the forward reaction rate to the reverse reaction rate [2], was kept constant. Since the concentration of each species at equilibrium is only determined by the affinity and the receptor-ligand separation [2], the observation of these two types of dependency is likely due to the kinetics, rather than the equilibrium of the receptor-ligand reaction. The saturation of the maximum adhesion force may be explained by the relatively constant adhesive zone profile and bond density. An illustration of the deformed profile of the cell membrane and contact zone profile is shown in Fig. 7. If the reaction is fast, the adhesion zone profile and the bond density are able to reach equilibrium almost instantaneously at any indentation depth. Since the adhesion force is only dependent on the adhesion zone profile and bond density, the maximum adhesion force is insensitive to the indentation depth for this scenario. If the response of the receptor-ligand bond formation is sluggish, however, bonds, which do not form instantaneously, may form at a later stage, thus contributing to the adhesion force subsequently. This kinetic effect explains why the maximum adhesion force during the retraction process depends on the maximum indentation depth.

Our simulation results also showed that the maximum adhesion force of a viscoelastic cell is sensitive to the maximum indentation depth even if a high receptor-ligand reaction rate is used. This can be clearly seen from Fig. 8 with $k_f^0=1.0\times10^2$ s^{-1} μm^2 and $k_r^0=1.0\times10^{-2}$ s^{-1}. This depen-

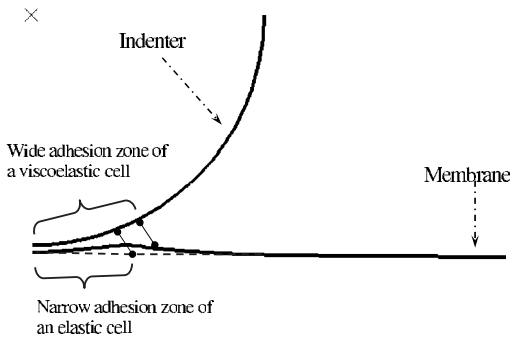

FIG. 9. Comparison between the deformed profiles of a viscoelastic cell (solid line) and an elastic cell (dashed line).

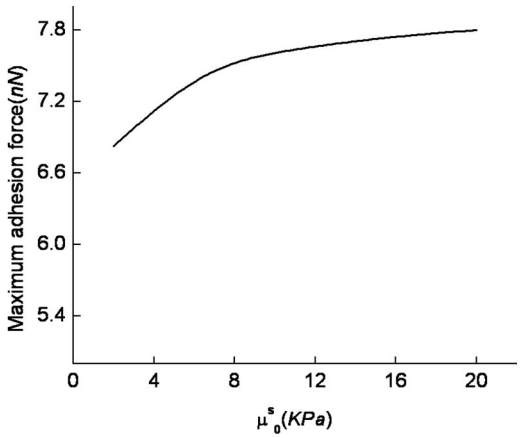

FIG. 10. Maximum adhesion force increases with the stiffness of a viscoelastic cell. $\mu_0^s=2.0-20.0$ K Pa, $\bar{\mu}_1=0.9$, and $\tau_1=1.0$ s.

dency may be attributed to cell viscoelasticity, which makes the cell response sluggish to deformation, similar to the sluggishness due to bond formation or breakage.

D. Influence of mechanical properties of cells on adhesion force

It was found that the adhesion force of a viscoelastic cell [hollow squares in Fig. 3(a)] was larger than that of an elastic cell with the same initial shear modulus [hollow triangles in Fig. 3(a)]. This difference may be attributed to the fact that the deformed profile of the viscoelastic cell is more conformable with the geometry of the indenter (Fig. 9). Therefore the adhesion zone as well as the adhesion force of the viscoelastic cell is larger than that of the elastic cell.

It was also found that the adhesion force of the stiff elastic cell [hollow circles in Fig. 3(a)] was slightly larger than that of the soft elastic cell [hollow triangles in Fig. 3(a)]. A similar observation was also found for the viscoelastic cells (Fig. 10). The influence of the mechanical properties of cells on the adhesion force may be understood by an idealized model, i.e., two Hookean springs were connected in a series [11,36–39]. In this model, one spring may represent the cell and the other may represent the receptor-ligand bonds, and the deformations in the two springs are coupled. Suppose the spring chain is elongated at a given rate. If one spring (say, the one representing the cell) becomes stiffer, its elongation rate becomes smaller while the elongation rate of the other spring (i.e., the one representing receptor-ligand bonds) has to be larger. As a consequence, the adhesion force of the receptor-ligand bonds becomes larger. However, when the spring representing the cell becomes too stiff (in the present simulations, $\mu_0^s>10.0$ K Pa), the elongation rate as well as the adhesion strength of the receptor-ligand spring becomes insensitive to the stiffness of the first spring.

IV. SUMMARY

A continuum-kinetics model was formulated to study the receptor-ligand mediated adhesion in the indentation of cells. It was found that in the presence of adhesion, the indentation loading and unloading curves may be influenced by the receptor-ligand reaction rate. The influence is significant at a high receptor-ligand reaction rate while insignificant at a low reaction rate. It was found that the adhesion force tilts the unloading curve downward and causes a larger hysteresis. The dependency of the adhesion force on the indentation rate is controlled by the receptor-ligand reaction rate. For a high reaction rate, the maximum adhesion force increases with the indentation rate while for a low reaction rate, the maximum adhesion force decreases with the indentation rate. Our calculation results also show that the maximum adhesion force increases with the indenter size. At a low reaction rate, the adhesion force of an elastic cell increases with the indentation depth while it saturates at a high reaction rate. For a viscoelastic cell, however, the adhesion force increases with the indentation depth even at a high reaction rate due to the cell viscoelasticity. Compared with an elastic cell at the same indentation depth, a viscoelastic cell produces a larger adhesion force due to the viscous deformation of the cell. With an increase in the stiffness of cells, the cell adhesion force may increase. However, when the cell becomes too stiff, the cell adhesion force saturates.

[1] G. Bao and S. Suresh, Nat. Mater. **2**, 715 (2003).
[2] C. E. Orsello, D. A. Lauffenburger, and D. A. Hammer, Trends Biotechnol. **19**, 310 (2001).
[3] E. A. Hassan, W. F. Heinz, M. D. Antonik, N. P. D' Costa, S. Nageswaran, C. A. Schoenenberger, and J. H. Hoh, Biophys. J. **74**, 1564 (1998).
[4] M. Sato, K. Nagayama, N. Kataoka, M. Sasaki, and K. Hane, J. Biomech. **33**, 127 (2000).
[5] A. B. Mathur, A. M. Collinsworth, W. M. Reichert, W. E. Kraus, and G. A. Truskey, J. Biomech. **34**, 1545 (2001).
[6] G. Sagvolden, I. Giaever, E. O. Pettersen, and J. Feder, Proc. Natl. Acad. Sci. U.S.A. **96**, 471 (1999).
[7] E. L. Florin, V. T. Moy, and H. E. Gaub, Science **264**, 415 (1994).

[8] C. E. McNamee, N. Pyo, S. Tanaka, I. U. Vakarelski, Y. Kanda, and K. Higashitani, Colloids Surf., B **48**, 176 (2006).
[9] H. Hertz, J. Reine Angew. Math. **92**, 156 (1881).
[10] I. N. Sneddon, Int. J. Eng. Sci. **3**, 47 (1965).
[11] G. I. Bell, Science **200**, 618 (1978).
[12] E. A. Evans, Biophys. J. **48**, 175 (1985).
[13] D. A. Hammer and D. A. Lauffenburger, Biophys. J. **52**, 475 (1987).
[14] M. Dembo, D. C. Torney, K. Saxaman, and D. A. Hammer, Proc. R. Soc. London, Ser. B **234**, 55 (1988).
[15] C. Zhu, J. Biomech. **33**, 23 (2000).
[16] D. A. Hammer and S. M. Apte, Biophys. J. **63**, 35 (1992).
[17] C. Dong and X. X. Lei, J. Biomech. **33**, 35 (2000).
[18] W. Shyy, M. Francois, H. S. Udaykumar, N. N'Dri, and R. Tran-Son-Tay, Appl. Mech. Rev. **54**, 405 (2001).
[19] N. A. N'Dri, W. Shyy, and R. Tran-Son-Tay, Biophys. J. **85**, 2273 (2003).
[20] K. E. Caputo and D. A. Hammer, Biophys. J. **89**, 187 (2005).
[21] D. Shin and K. Athanasiou, J. Orthop. Res. **17**, 880 (1999).
[22] S. Yamada, D. Wirtz, and S. C. Kuo, Biophys. J. **78**, 1736 (2000).
[23] E. J. Koay, A. C. Sheih, and K. A. Athanasiou, ASME J. Biomech. Eng. **125**, 334 (2003).
[24] F. Guilak and V. Mow, J. Biomech. **33**, 1663 (2000).
[25] L. Setton, W. Zhu, and V. Mow, J. Biomech. **26**, 581 (1993).
[26] P. Fernández, P. A. Pullarkat, and A. Ott, Biophys. J. **90**, 3796 (2006).
[27] F. P. T. Baaijens, W. R. Trickey, T. A. Laursen, and F. Guilak, Ann. Biomed. Eng. **33**, 494 (2005).
[28] M. Dao, C. T. Lim, and S. Suresh, J. Mech. Phys. Solids **51**, 2259 (2003).
[29] C. T. Lim, M. Dao, S. Suresh, C. H. Sow, and K. T. Chew, Acta Mater. **52**, 1837 (2004).
[30] K. C. Chang and D. A. Hammer, Langmuir **12**, 2271 (1996).
[31] *ABAQUS Theory Manual, Version 6.6* (ABAQUS Inc., Providence, RI, 2006).
[32] R. E. Mahaffy, C. K. Shih, F. C. MacKintosh, and J. Käs, Phys. Rev. Lett. **85**, 880 (2000).
[33] C. Bustamante, J. F. Marko, E. D. Siggia, and S. Smith, Science **265**, 1599 (1994).
[34] N. Yu, W. A. Bonin, and A. A. Polycarpou, Rev. Sci. Instrum. **76**, 045109 (2005).
[35] H.-J. Butt, Biophys. J. **60**, 777 (1991).
[36] E. Evans and K. Ritchie, Biophys. J. **72**, 1541 (1997).
[37] U. Seifert, Phys. Rev. Lett. **84**, 2750 (2000).
[38] B. Heymann and H. Grubmüller, Phys. Rev. Lett. **84**, 6126 (2000).
[39] G. Hummer and A. Szabo, Biophys. J. **85**, 5 (2003).